BIOLOGICAL FUNCTIONS OF LOW-FREQUENCY VIBRATIONS (PHONONS)

III. Helical Structures and Microenvironment

KUO-CHEN CHOU
Baker Laboratory of Chemistry, Cornell University, Ithaca, New York 14853

ABSTRACT Low-frequency vibrations in biomacromolecules possess significant biological functions. In this paper, the α-helix element is compared with a mass-distributed spring. Based on this, a set of intuitive and easily handled equations are derived for predicting the fundamental frequencies of helical structures in protein molecules. As shown in the equations, the fundamental frequency depends not only on the constituents of a helix itself but also on its microenvironment. The calculated results agree with the observations. The calculations also demonstrate that the low-frequency vibrations with wave number of $\sim 30\ cm^{-1}$ do not necessarily arise from motions that involve either all or very large portions of the protein molecule as previously thought; a piece of helix containing more than 10 residues and surrounded by a proper microenvironment can also generate such low-frequency motions. Furthermore, we illustrate that the low-frequency motions are closely related to the native state of a protein molecule. Upon denaturation, which is accompanied by a radical change of the relevant microenvironment, the original fundamental frequency also disappears. Consequently, this kind of special frequency termed activating low frequency can serve as a dynamic criteron in identifying whether a biomacromolecule is in its native state. The energy of a phonon excited by this kind of low-frequency vibration is of the same order of magnitude as the average enthalpy value per residue measured during conformational change in some protein molecules. Therefore, there must be some intrinsic relation between the allosteric transitions of protein molecules and their low-frequency motions.

INTRODUCTION

With the emergence of a series of experimental results (1–7) showing the existence of low-frequency motions in biomacromolecules, more attention has been recently paid to the biological functions of low-frequency vibrations in proteins and other biomacromolecules. They can roughly be classified as follows. (*a*) Green (8), Ji (9), and Fröhlich (10) envisioned that the low-frequency pulsation, which involves either all or large portions of a protein molecule, might play a critical role in the catalytic function of enzyme. (*b*) Suezaki and Gō (11), and Ponnuswamy and Bhaskaran (12) treated globular proteins as continuous elastic spheres or as prolate and oblate spheroidal bodies, and described their low-frequency breathing motions. (*c*) Careri et al. (13) and Englander (14) studied the relationship between the hydrogen exchange properties and this kind of internal motion in proteins and nucleic acids. (*d*) Chou and Chen (15) demonstrated that the associations between some biomacromolecules would concomitantly excite low-frequency phonons (whose wave numbers are 10–100 cm^{-1}), otherwise a thermodynamic deficit could not be compensated for. Based on such a thermodynamic deduction, the relationship between this kind of low-frequency vibration and the conformational changes in biomacromolecules are discussed. (*e*) Sobell et al. (16–18) presumed that the low-frequency (acoustic) phonons can play an important role in DNA breathing and drug intercalation. (*f*) Zhou (19) investigated the vibrational energy of a ringlike DNA and analyzed related biophysical phenomena. (*g*) Chou et al. (20) discussed the relationship between low-frequency vibrations and the cooperative effects in oligomeric proteins. Based on this, a physical picture describing the microscopic mechanism of the cooperativity in hemoglobin was shown.

Now that the low-frequency vibrations do really exist in biomacromolecules and reveal significant biological functions, the following questions are naturally raised. (*a*) How do we calculate or predict this kind of low-frequency motions from a known component element in a biomacromolecule? (*b*) How does the microenvironment around the component element influence its fundamental frequency (lowest frequency)? (*c*) What is the inherent relation between this kind of fundamental frequency in a biomacromolecule and its biological function? The present study was initiated in an attempt to approach these basic subjects. Because the α-helices occupy a prominent posi-

Dr. Chou is a visiting professor from Shanghai Institute of Biochemistry, Chinese Academy of Sciences.

tion among the component elements of protein molecules, we will take the α-helical structure element as a typical subject and attempt to carry out an investigation.

CONTINUITY MODEL AND CALCULATION FORMULAE

Due to the extreme complexity and inherent flexibility of biomacromolecules, rather than the discrete model suitable for the normal mode calculation method developed by Wilson (21), Itoh et al. (22), and Fanconi et al. (23), we prefer to adopt the continuity model to treat the internal low-frequency motions in biomacromolecules. In principle, the normal mode calculation method can be used to calculate and analyze vibrational movements in any molecules, but in practice this is unfortunately computationally impossible due to the lack of symmetry in biomacromolecules and limitations on computer size and speed. When discussing the high-frequency vibrations of a molecule, which involve very small relative displacements and very strong molecular forces (such as covalent bonds) between neighbor individual atoms, one must resort to a discrete model. But for the low-frequency motions in a biomacromolecule, which involve much larger effective masses and much weaker force constants (15), and whose modes can be compared with an accordionlike motion (1), heartbeat pulsation (8–9), or any kind of vibration that involves many atoms and spans a much bigger dimension than the length of a covalent bond, it is not only more convenient but also physically reasonable to use the continuity model. A similar concept regarding the continuity model was also described by Suezaki and Gō (11), and Ponnuswamy and Bhaskaran (12). In adopting the continuity model, one will of course lose the information concerning the high-frequency motions in a biomacromolecule. Nevertheless, this is worthwhile because the low-frequency motions in a biomacromolecule possess much more significant biological functions than the high-frequency motions (8–9, 13–20). Besides by means of the continuity model, we can easily obtain an intuitive and clear physical picture of low-frequency vibrations in a biomacromolecule, which is very helpful in gaining an insight into their biological functions.

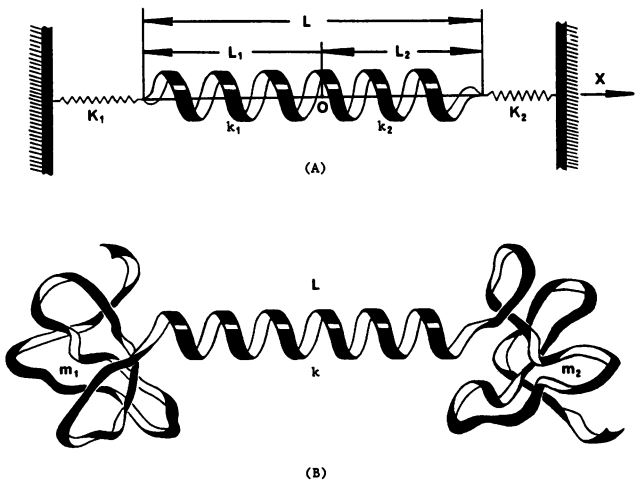

FIGURE 1 The vibration system of the helical structure in which the two ends of a helix are linked to (*A*) two mass-negligible springs with force constants K_1 and K_2, respectively, and (*B*) two sequential fragments with mass m_1 and m_2.

According to the continuity model, an α-helix can be compared with a spring whose mass, however, is not negligible, namely, to a spring with distributed mass. Based on this, the fundamental frequencies of a helix with different terminal conditions can be expressed as follows (see Appendix I). (*a*) If the two ends of a helix are linked to two mass-negligible springs as illustrated in Fig. 1 *A*, then we have

$$\tilde{\nu} = \frac{\nu}{c} = \frac{1}{2\pi c}\left[\frac{k + K^*}{(\alpha_1^3 + \alpha_2^3)\rho L/3}\right]^{1/2} \tag{1}$$

with

$$\alpha_1 = \frac{K_2}{K_1 + K_2}, \qquad \alpha_2 = \frac{K_1}{K_1 + K_2} \tag{2}$$

$$K^* = \frac{K_1 K_2}{K_1 + K_2}, \tag{3}$$

where ν is the fundamental frequency of the system considered, $\tilde{\nu}$ the corresponding wave number, c the speed of light, k the stretching force constant of the helix, ρ the mass per unit length along the axis of the helix, L the length of the helical axis, and K_1 and K_2 are the force constants of the two attached mass-negligible springs, respectively. (*b*) If the two ends of the helix are linked to two fragments with masses m_1 and m_2 (Fig. 1 *B*), respectively, then we instead have

$$\tilde{\nu} = \frac{\nu}{c} = \frac{1}{2\pi c}\left[\frac{k}{m^* + (\beta_1^3 + \beta_2^3)\rho L/3}\right]^{1/2} \tag{4}$$

with

$$\beta_1 = \frac{m_2}{m_1 + m_2}, \qquad \beta_2 = \frac{m_1}{m_1 + m_2} \tag{5}$$

$$m^* = \frac{m_1 m_2}{m_1 + m_2}. \tag{6}$$

From above we see that to calculate the fundamental frequency of a helix system we have to find the stretching force constant of the helix. Obviously, for an α-helix being in an accordionlike vibration, its force constant is essentially related to the constituent hydrogen bonds. As is well-known, the normal α-helix has 3.6 residues per turn, with a hydrogen bond between the CO of the i^{th} residue and the NH of the $(i + 4)^{\text{th}}$ residue as shown in Fig. 2. Now, the problem is how to express the stretching force constant of the whole α-helix in terms of the force constants of the

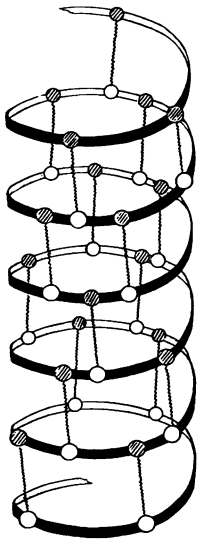

FIGURE 2 Illustration of an α-helix where ○ denotes peptide oxygen, and ⊘ peptide nitrogen, and ∿∿∿ denotes hydrogen bond.

constituent hydrogen bonds. For such a purpose, it would be instructive to further compare an α-helix with a cylinder, then imagine that its flank is cut off along a straight line parallel to the helix axis, and flattened as illustrated in Fig. 3. Because the hydrogen bonds in an α-helix are not precisely parallel to the helix axis, but have some deviation angle, say θ, from it, the following step referring to the

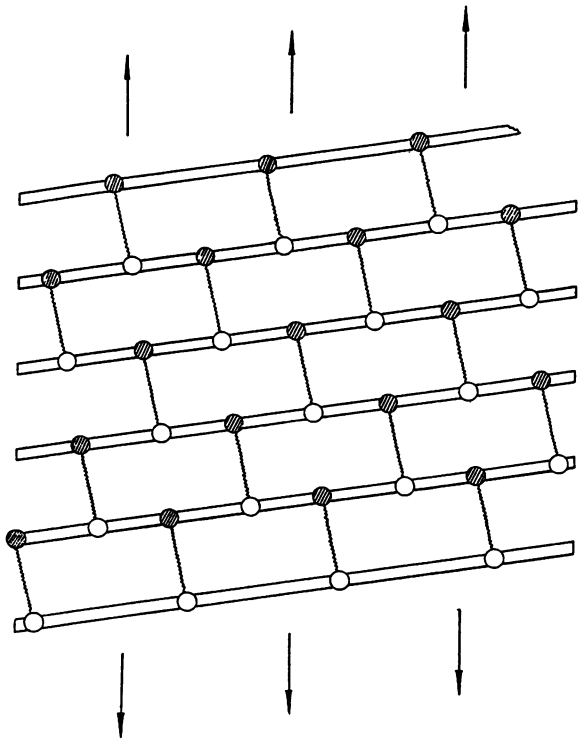

FIGURE 3 Illustration obtained by cutting and flattening the flank of the α-helix in Fig. 2.

resolution and composition of force constants is necessary. Suppose the stretching and bending force constants of the hydrogen bond are k_S^H and k_B^H, respectively. Then the force constant for such a hydrogen bond vibrating along the helix axis should be

$$k_H^* = [(k_H^S \cos\theta)^2 + (k_H^B \sin\theta)^2]^{1/2}. \quad (7)$$

Thus, according to the combination relations of force constants as given in Appendix II, the resultant force constant, k, for the spring system as shown in Fig. 3 can be expressed as

$$k = [(1/4k_H^*) + (1/4k_H^*) + (1/3k_H^*) + (1/4k_H^*) + (1/3k_H^*)]^{-1}. \quad (8)$$

Following the above steps, for any α-helix, we can always derive the approximate expression of its stretching force constant in terms of the force constants of the constituent hydrogen bonds, e.g., for a normal α-helix with 11 amino-acid residues, the corresponding stretching force constant is

$$k = [(1/4k_H^*) + (1/3k_H^*)]^{-1} = \frac{12}{7} k_H^*. \quad (9)$$

Note that the number of the hydrogen bonds in an α-helix is generally $n - 4$, where n is the number of the constituent amino-acid residues.

FUNDAMENTAL FREQUENCY AND MICROENVIRONMENTS

The observations by laser Raman spectroscopy (1) show the pronounced low-frequency peaks at ~29 cm^{-1} and 32 cm^{-1} for α-chymotrypsin and pepsin, respectively. However, upon denaturation their respective low-frequency peaks disappear, too, which means this kind of low-frequency vibration is very sensitive to the conformations of protein molecules. To explain the above experimental results, Suezaki and Gō (11) likened the native globular proteins to continuous elastic spheres in low-frequency breathing motions and used the formula

$$\tilde{\nu} = \frac{1}{2\pi c}\left(\frac{\pi E}{\rho r^2}\right)^{1/2} \quad (10)$$

to calculate their wave numbers. In Eq. 10, E is Young's modulus of the elastic material, and ρ and r are the mass density and radius of the sphere, respectively. They substituted $E = 10^{11}$ dyn/cm^2, $r = 20$ Å, and $\rho = 1$ g/cm^3 into Eq. 10 and obtained $\tilde{\nu} = 26$ cm^{-1}. However, the validity of their calculations might be questioned for the following reasons. First, there is no reliable information about the value of E for globular proteins, and the value they took was rather arbitrary. Second, their calculations did not touch on any specific character of internal structures of individual protein molecules. According to their model, the low-frequency wave number should be inversely propor-

tional to the size of the protein molecule no matter what conformation it has (see Eq. 10). Obviously, there is not such a simple relation in actual observations. Furthermore, for some proteins, e.g., carboxypeptidase, so far even a weak low-frequency peak has not been observed (1). All these indicate that the low-frequency modes apparently hinge on the internal structures of protein molecules. Now, let us investigate these phenomena according to the internal structures of protein molecules.

α-Chymotrypsin

α-chymotrypsin consists of 245 residues. A view of its complete polypeptide chain is outlined in Fig. 4, where residues 57, 102, and 195 are the components of the active site (24). The β-barrel 1, formed by six adjacent anti-parallel chains along the sequence from residues 29 to 112, appears at the upper left; while the β-barrel 2, formed also by six adjacent anti-parallel chains from residues 133 to 230, is at the lower right. There are three α-helices. Helix 1 involves residues 164 to 179, and hence is entirely bound in the β-barrel 2. Therefore, it is not likely that there is any low-frequency vibration coming from this helix, which is seriously restricted by the surroundings. Helix 2 (residues 230–235) and helix 3 (residues 235–245) are contiguous to each other, and their axes make an angle of ~40°. But helix 2 is almost buried inside the molecule, too. Accordingly, only helix 3, the COOH-terminal α-helix, is on the enzyme surface, forming a tail on the second barrel and making hydrophobic contacts with both barrels. Besides, the only hydrogen bond between the COOH-terminal helix and the remainder of the molecule is a salt bridge from the terminal carboxyl group to Lys 107, and such a hydrogen bond is almost perpendicular to the COOH-terminal helix axis. The other end of the COOH-terminal helix is linked by a covalent bond to helix 2, which, however, is buried inside the protein molecule, therefore this end is actually linked by a covalent bond to an object whose mass is much bigger than that of the COOH-terminal helix. Because both the covalent bond and hydrogen bond can be regarded as mass-negligible springs, the COOH-terminal helix plus its microenvironment, as described above, can be classified to the category of vibration system illustrated in Fig. 1 *A*. But note that in the case considered here, one of the two mass-negligible springs is linked to the helix in a mutually perpendicular way. Therefore, for this spring, rather than stretching force constant, we should take the corresponding bending force constant for calculation. For example, in Eqs. 2–3, we should assign,

$$K_1 = k_C^S, \qquad K_2 = k_H^B, \tag{11}$$

where k_C^S is the stretching force constant of a covalent bond, while k_H^B has the same implication as in Eq. 7.

The amino-acid sequence of the COOH-terminal helix is (24)

Val-Asn-Trp-Val-Gln-Gln-Thr-Leu-Ala-Ala-Asn
(235) (245)

whose mass is 1,242 daltons. To make a fair approximation, we can suppose ρ, the mass per unit length of the helix, is even, and thus have

$$\rho L = \frac{1{,}242}{N} \text{ grams}, \tag{12}$$

where N is the Avogadro constant.

The stretching force constant of the helix can be calculated by means of the method described in the last section. For a helix with 11 residues, the expression of its stretching force constant has already been given in Eq. 9. The stretching force constant, k_H^S, of the hydrogen bond is 0.13×10^5 dyn/cm, and its bending force constant k_H^B is 0.03×10^5 dyn/cm (24). The deviation angle, θ, of the hydrogen bonds from the helix axis is 2 26°. Then accord-

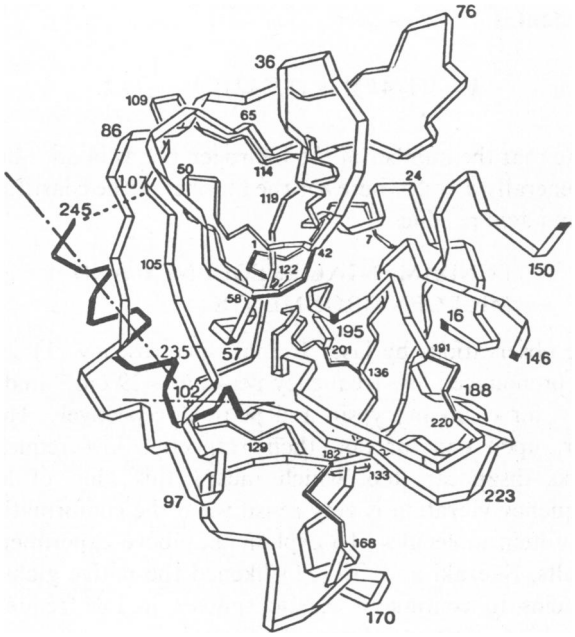

FIGURE 4 A view of α-chymotrypsin, where the polypeptide chain is represented by a ribbon folded at each α-carbon atom. Helix 1, the COOH-terminal α-helix (residues 235–245) is on the enzyme surface, and the short contiguous helix 2 (residues 230–235) are almost buried inside the protein molecule. These two helices are specially marked by dark color. Their axes (indicated by —— · ——) makes an angle of ~40°. Helix 1 (residues 164–179) is wholly bound in β-barrel 2 (residues 133–230), which is located at the lower right of the figure. β-barrel 1 (residues 29–112) appears at the upper left, in front of the COOH-terminal helix. It looks like that the COOH-terminal helix forms a tail on the second cylinder (β-barrel) and makes hydrophobic contacts with both cylinders (β-barrels 1 and 2). The only hydrogen bond between COOH-terminal helix and the remainder of the protein molecule is that made by the terminal carboxyl group with Lys 107 (illustrated by ---) holding the COOH-terminal helix more firmly to the enzyme surface. Residues 57, 102, and 195 are the components of the active site. Disulphide linkages are indicated by shaded bars.

ing to Eq. 7

$$k_H^* = [(0.13 \cos 26°)^2 + (0.03 \sin 26°)^2]^{1/2} \times 10^5$$
$$= 0.12 \times 10^5 \text{ dyn/cm.} \quad (13)$$

Substitution of the above into Eq. 9 gives

$$k = 0.20 \times 10^5 \text{ dyn/cm.} \quad (14)$$

Because the force constant of a covalent bond is much larger than that of a hydrogen bond, Eqs. 2–3 can be reduced to (cf. Eq. 11)

$$\alpha_1 \simeq 0, \qquad \alpha_2 \simeq 1 \quad (15)$$

$$K^* \simeq k_H^B = 0.03 \times 10^5 \text{ dyn/cm.} \quad (16)$$

Substituting Eqs. 14–16 into Eq. 1, we obtain

$$\tilde{\nu} = \frac{1}{2\pi \times 3 \times 10^{10}} \left[\frac{(0.20 + 0.03) \times 10^5 \times 6.02 \times 10^{23}}{\frac{1,242}{3}} \right]^{1/2}$$
$$= 30 \text{ cm}^{-1}, \quad (17)$$

which is in good agreement with the result observed by Brown et al. (1).

However, when the α-chymotrypsin was denatured with sodium dodecyl sulfate, the salt bridge between Lys 107 and Asn 245 (Fig. 4) was disrupted as well, and hence the one end of the COOH-terminal helix is no longer held to the enzyme surface. In this case the low-frequency peak at 29 cm^{-1}, which is closely related to the conformation before denaturation as illustrated in the aforementioned calculation, will of course vanish. Instead, "rather intense Raman scattering throughout the region of 20–150 cm^{-1} is observed on the denatured material, but it is broad and structureless," as described by Brown et al. (1). This is apparently related to the free motion of the one end of the COOH-terminal helix, which will no doubt increase the background noise, and also related to a decrease in the order of protein conformation. Furthermore, the hydrophobic contact of the COOH-terminal helix with both β-barrel 1 and β-barrel 2, which somewhat plays a role in stabilizing the relative position of the two β-barrels, will also be collapsed. This will automatically be followed by a change of the relative positions among the active groups His 57, Asp 102, and Ser 195 (Fig. 4), and eventually result in a loss of activity.

Pepsin

Pepsin has 327 residues (25). Those stretches of polypeptide chain that adopt a helical conformation are residues 58–62, 137–141, 225–235, and 303–309 (26). Among these four helices, only the helix (residues 225–235) is most likely related to the observed low-frequency peak of 32 cm^{-1} (1) because the other three helices are too short,

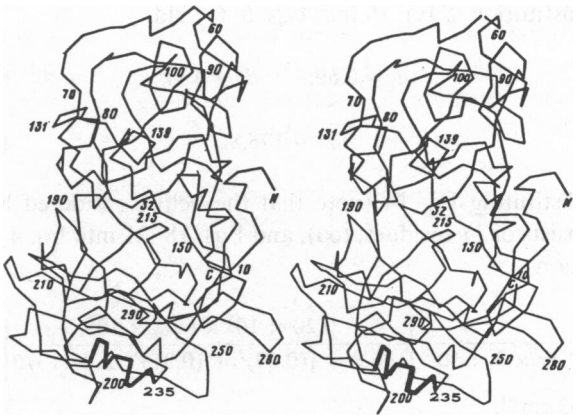

FIGURE 5 Stereoscopic drawing of the pepsin polypeptide chain constructed on the basis of the coordinates of the α-carbon atoms. The helix (residues 225–235) is drawn with bold-darkened line. The two sequential segments, residues 222–224 and residues 236–241, are linked along the sequence to the two ends of the helix (residues 225–235). But both these segments have some free space to vibrate with very weak constraints from the other joint parts of the sequence, and hence can be approximately treated as two attached mass fragments as illustrated in Fig. 1 *B*.

consisting merely of four to six residues. Besides, this helix is situated on the surface of the enzyme as can be seen from Fig. 5, the stereoscopic drawing of the pepsin polypeptide chain based on the α-carbon atoms (27). For clarity, in Fig. 5 the helix (residues 225–235) is marked by a thick line. The two ends of the helix are linked by covalent bonds to two segments (residues 222–224 and residues 236–241) that both of them have some free space and can vibrate along the helix axis but undergo very weak constraints from the other joint part of the sequence. They can therefore be approximately treated as two mass fragments, attached to the two ends of the helix, as shown in Fig. 1 *B*. Consequently, the microenvironment in the present case makes the helix (residues 225–235) belong to the category of vibration systems as described by Fig. 1 *B*. In other words, its fundamental frequency should be calculated by Eq. 4.

The amino-acid sequence of the helix is (25)

Thr-Ser-Ala-Ile-Ala-Ile-Asn-Ile-Gln-Ser-Asp,
(225) (235)

which gives

$$\rho L = 1,113 \text{ daltons} = \frac{1,113}{N} \text{ grams.} \quad (18)$$

The residues 222–224 and 236–241 that attach to the two ends of the above helix and can be approximately regarded as two mass fragments are Thr-Gly-Pro and Ile-Gly-Ala-Ser-Glu-Asn, respectively. Therefore we have

$$m_1 = \frac{256}{N} \text{ grams,} \qquad m_2 = \frac{571}{N} \text{ grams.} \quad (19)$$

Substitution of Eq. 19 into Eqs. 5–6 yields

$$\beta_1 = 0.69, \qquad \beta_2 = 0.31 \tag{20}$$

$$m^* = 176.8. \tag{21}$$

Substituting Eq. 14 (note that the helix considered here consists of 11 residues, too), and Eqs. 18–21 into Eq. 4, we obtain

$$\tilde{\nu} = \frac{1}{2\pi \times 3 \times 10^{10}} \left\{ \frac{0.20 \times 10^5 \times 6.02 \times 10^{23}}{176.8 + [(0.69)^3 + (0.31)^3] \times 1{,}113/3} \right\}^{1/2}$$
$$= 33 \text{ cm}^{-1}, \tag{22}$$

which is also in good agreement with the observed value of 32 cm^{-1} (1).

Recently, Gō et al. (30) made an interesting computation for a small globular protein, the bovine pancreatic trypsin inhibitor, by treating the energy surface as a multidimensional parabola and only dihedral angles as variables. According to such an approach they found a frequency spectrum, among which, however, the lowest frequency is 5.7 cm^{-1}, ~15–30 cm^{-1} lower than the lowest frequencies so far observed for most globular proteins (31). Besides, it is also a question how to single out from the frequency spectrum the dominant low frequency that corresponds to the outstanding low-frequency peak observed uniquely, and how to give such a dominant low-frequency motion an intuitive physical picture.

LOW-FREQUENCY AMPLITUDE

As is well-known, an oscillator with frequency ν will excite the phonons with energy of $h\nu$. Because phonons are bosons (15), under thermal equilibrium, the mean number of phonons thus excited is, according to Bose-Einstein statistics, given by

$$\langle n \rangle = \frac{1}{e^{h\nu/k_B T} - 1}, \tag{23}$$

where k_B is the Boltzmann constant, h the Planck constant, and T the absolute temperature. Therefore, the average vibration energy of the oscillator is

$$\langle E \rangle = \langle n \rangle h\nu = \frac{h\nu}{e^{h\nu/k_B T} - 1}. \tag{24}$$

On the other hand, a combination of Eqs. A12, A6, A7, and 2 and 3 will give

$$\text{Max } U = [(\alpha_1 k + \alpha_1^2 K_1) + (\alpha_2 k + \alpha_2^2 K_2)]\sigma^2/2$$
$$= (k + K^*)\sigma^2/2. \tag{25}$$

According to energy conservation, we have Max $U = \langle E \rangle$ and therefore the amplitude can be written as

$$\sigma = \sqrt{\frac{2h\nu/(e^{h\nu/k_B T} - 1)}{k + K^*}}\Bigg|_{h\nu \ll k_B T}$$
$$\simeq \sqrt{\frac{2k_B T}{k + K^*}}. \tag{26}$$

Note that, for low-frequency phonons whose wave numbers are <50 cm^{-1}, we generally have $h\nu \ll k_B T$ at room temperature. Now for the COOH-terminal α-helix (residues 235–245) of a α-chymotrypsin, substituting T = 300°K, $k = 0.20 \times 10^5$ dyn/cm and $K^* = 0.03 \times 10^5$ dyn/cm (see Eqs. 14 and 16) into Eq. 26, we obtain σ = 0.20 Å. Similarly, for the helix (residues 225–235) in pepsin we have σ = 0.21 Å at room temperature (note that in this case $K^* = 0$). Therefore, at room temperature the low-frequency amplitudes thus calculated for the two α-helices each having 11 amino-acid residues are in good agreement with the room mean square (rms) displacement of the overall end-to-end length found by Peticolas (28) for an essentially same helical structure.

LOW-FREQUENCY VIBRATIONS AND BIOLOGICAL FUNCTIONS

From the above illustrations, we can see how the fundamental frequency of a helix in a protein molecule depends on its microenvironment as well as the constituents of itself. On the other hand, this kind of low-frequency vibration is also closely related to the native state of a protein molecule. As observed upon denaturation, the original low-frequency modes existing in α-chymotrypsin and pepsin disappear immediately (1). According to the above theoretical analysis, this can be attributed to a conformational change of the protein molecules, which of course includes a dramatic change of the relevant microenvironments. Consequently, both the experimental observation and the theoretical analysis would naturally yield the concept of activating low frequency (20), which possesses a unique character and might serve as a potential dynamic criterion for identifying whether a biomacromolecule is in its activated state, because the creation and annihilation of such low-frequency phonons are always accompanied by a major conformational change in a protein molecule, which is actually closely related to its activation and deactivation. Furthermore, the idea of activating low frequency will be very useful for investigating the action mechanism of biomacromolecules from the viewpoint of dynamics (8–9, 15, 20).

Note that, the energy, $h\nu$, of a phonon excited by this kind of low-frequency vibrations is ~85 cal/mol. But when pepsin undergoes conformational change of denaturation, the measured enthalpy is 22 kcal/mol (29). Dividing the above value by 327, the number of residues in pepsin, we obtain ~67 cal/mol, the corresponding enthalpy for each

residue in average. Therefore the low-frequency phonon energy possesses the same order of magnitude as the average enthalpy value measured for each residue during conformational changes in some protein molecules. Accordingly, it is very likely that this kind of low-frequency vibration can describe the microscopic process and mechanism of the allosteric transition in a protein molecule and the transmission of biological information at the molecular level. Further investigation and the related details on this subject will be presented in another report.

CONCLUSIONS

The fundamental frequencies calculated with the formulae derived in this paper are in good agreement with the experimental results. As reflected in our formulae, the fundamental frequency of a helix is related not only to the constituents of itself, but also to its microenvironment, and thereby to the conformation of a whole protein molecule.

Our calculated results also show that the low-frequency vibrations with wave numbers of $\sim 30\ cm^{-1}$ do not necessarily arise from motions that involve "either all or very large portions" of the protein molecules as suggested by Brown et al. (1). A piece of helix containing more than 10 residues plus a proper microenvironment can also generate this kind of low-frequency vibration. Such a conclusion is also supported by the rigorous normal mode calculations, in which a more simple and ideal α-helix of poly-L-alanine was taken as the model (22). When the number of the constituent alanine residues is 15, the wave number of the corresponding fundamental frequency thus obtained is 29 cm^{-1}. This indicates good agreement between the results obtained by our calculations and by the rigorous normal mode method if a reasonable factor regarding the differences in both the end conditions and the constituents of the helices is taken into account. Besides, our calculated results in both the fundamental frequencies and the corresponding low-frequency amplitudes are also supported by a recent paper of Peticolas (28), who applied an adjustable parameter to simplify calculations and obtained some quite interesting results as well.

Although the calculated results based on such a consideration are in good agreement with the observations, generally speaking, there might exist different vibrational modes for different protein molecules, depending on individual internal structures. For example, a low-frequency peak was also observed for immunoglobulin G, whose conformation assumes extensive β-sheet regions but no α-helical regions at all. Therefore, as a further step, an investigation into the fundamental vibrations of β-structure is necessary, and will be approached elsewhere.

APPENDIX I

The fundamental frequency of the vibration system illustrated in Fig. 1 *A* can be derived as follows. Suppose O is the static reference point of the vibrational system concerned. The two sides of this point will move always in an opposite direction. Such a point actually divides the spring L into two parts, L_1 and L_2 whose force constants are assumed to be k_1 and k_2, respectively.

If σ_1 and σ_2 are the maximum absolute displacements of the two ends of the spring L along the x-axis (Fig. 1 *A*), then according to the property of an even spring we obviously have

$$\frac{\sigma_1}{L_1} = \frac{\sigma_2}{L_2} \tag{A1}$$

with

$$L = L_1 + L_2$$

$$\sigma = \sigma_1 + \sigma_2, \tag{A2}$$

where σ is the maximum stretch amount of the spring L. Suppose the force constant of the spring is k, which can be written as (see Appendix II)

$$\frac{1}{k} = \frac{1}{k_1} + \frac{1}{k_2}, \tag{A3}$$

where k_1 and k_2 are the force constants of the springs L_1 and L_2, respectively. On the other hand, according to the force equilibrium of the system, we have

$$K_1\sigma_1 = K_2\sigma_2, \tag{A4}$$

where K_1 and K_2 are the force constants of the two mass-negligible springs linked to the two ends of the spring L, as shown in Fig. 1 *A*.

From Eqs. A1–A4, it follows

$$L_1 = \alpha_1 L$$

$$L_2 = \alpha_2 L \tag{A5}$$

$$\sigma_1 = \alpha_1 \sigma$$

$$\sigma_2 = \alpha_2 \sigma \tag{A6}$$

$$k_1 = \frac{k}{\alpha_1}$$

$$k_2 = \frac{k}{\alpha_2}, \tag{A7}$$

where α_1 and α_2 are defined as in Eq. 2. The displacements of any points on L_1 and L_2 at any time can be described by

$$u_1(x,t) = \frac{x}{L_1}\sigma_1 \sin \omega t \qquad (-L_1 \le x \le 0)$$

$$u_2(x,t) = \frac{x}{L_2}\sigma_2 \sin \omega t \qquad (0 \le x \le L_2) \tag{A8}$$

respectively, where ω is the round frequency. Suppose ρ is the mass per unit length of the mass-distributed spring, then the maximum kinetic energy of an element $\rho\Delta x$ of the spring L_1, a distance x_i from the point 0, is

$$\text{Max}\ (\Delta T_1^i) = \frac{\rho\Delta x}{2}\ \text{Max}\left[\frac{du_1}{dt}\right]_{x_i}^2 = \frac{\rho\Delta x}{2}\left[\frac{x_i}{L_1}\sigma_1\omega\right]^2. \tag{A9}$$

The total maximum kinetic energy of the spring L_1 is thus

$$\text{Max}\ T_1 = \lim_{\Delta x \to 0}\left[\sum_i \text{Max}\ (\Delta T_1^i)\right] = \frac{\rho}{2}\frac{\sigma_1^2\omega^2}{L_1}\int_0^{L_1} x^2 dx$$

$$= \rho L_1 \omega^2 \sigma_1^2/6. \tag{A10}$$

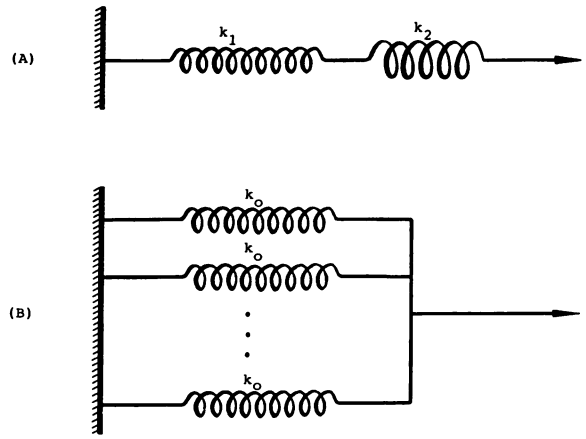

FIGURE 6 The spring system that is formed by (*A*) a series connection of two individual springs, and (*B*) a parallel connection of *n* identical springs.

Similarly, the total maximum kinetic energy of the spring L_2 is

$$\text{Max } T_2 = \rho L_2 \omega^2 \sigma_2^2/6. \tag{A11}$$

On the other hand, the total maximum potential energy of the whole spring system is

$$\begin{aligned}\text{Max } U &= \int_0^{\sigma_1} (k_1 + K_1)x'\mathrm{d}x' + \int_0^{\sigma_2} (k_2 + K_2)x'\mathrm{d}x' \\ &= (k_1 + K_1)\sigma_1^2/2 + (k_2 + K_2)\sigma_2^2/2.\end{aligned} \tag{A12}$$

According to energy conservation, we have

$$\text{Max } T_1 + \text{Max } T_2 = \text{Max } U \tag{A13}$$

or

$$\rho(L_1\sigma_1{}^2 + L_2\sigma_2^2)\omega^2/3 = (k_1 + K_1)\sigma_1^2 + (k_2 + K_2)\sigma_2^2. \tag{A14}$$

Substituting Eqs. A5–A7 into the above, we obtain

$$\omega^2(\alpha_1^3 + \alpha_2^3)\rho L/3 = (\alpha_1 + \alpha_2)k + \alpha_1^2 K_1 + \alpha_2^2 K_2, \tag{A15}$$

which yields

$$\omega = \left[\frac{k + K^*}{(\alpha_1^3 + \alpha_2^3)\rho L/3}\right]^{1/2}, \tag{A16}$$

where K^* is defined as in Eq. 3. Based on Eq. A16, the corresponding fundamental frequency and wave number can be expressed as in Eq. 1. Following the analogous derivation steps, we can obtain Eqs. 4–6.

APPENDIX II

Consider the force constant of the spring system shown in Fig. 6 *A*. Applying a unit force at its right end, each constituent spring will stretch by an amount $1/k_1$ and $1/k_2$, and the total displacement of the end becomes

$$\Delta L = \frac{1}{k_1} + \frac{1}{k_2}. \tag{A17}$$

By definition, the resultant force constant for the system should be

$$k = \frac{1}{\Delta L} = \frac{1}{\dfrac{1}{k_1} + \dfrac{1}{k_2}}. \tag{A18}$$

Generally speaking, for a system consisting of *n* springs in series connection, the resultant force constant, *k*, can be written as

$$k = \frac{1}{\dfrac{1}{k_2} + \dfrac{1}{k_2} + \cdots + \dfrac{1}{k_n}}, \tag{A19}$$

where k_1, k_2, ..., k_n are the force constants of the *n* individual springs, respectively.

However, if a spring system consists of *n* identical springs in parallel connection as illustrated in Fig. 6 *B*, a similar derivation will result

$$k = nk_o. \tag{A20}$$

Above we see that there is actually a crosswide corresponding relation between the formulae for calculating the resultant spring force constant and those for calculating the resultant resistance as far as the series connection and parallel connection are concerned.

Received for publication 26 July 1982 and in final form 19 December 1983.

REFERENCES

1. Brown, K. G, S. C. Erfurth, E. W. Small, and W. L. Peticolas. 1972. Conformationally dependent low-frequency motions of proteins by laser Raman spectroscopy. *Proc. Natl. Acad. Sci. USA.* 69:1467–1469.
2. Lakowicz, J. R., and G. Weber. 1973. Quenching of protein fluorescence by oxygen detection of structural fluctuations in proteins on the nanosecond time scale. *Biochemistry.* 12:4171–4179.
3. Saviotti, M. L., and W. C. Galley. 1974. Room temperature phosphorescence and the dynamic aspects of protein structure. *Proc. Natl. Acad. Sci. USA.* 71:4154–4158.
4. Hull, W. E., and B. D. Sykes. 1975. Fluorotyrosine alkaline phosphatase: internal internal mobility of individual tyrosines and the role of chemical shift anisotropy as a ^{19}F nuclear spin relaxation mechanism in proteins. *J. Mol. Biol.* 98:121–153.
5. Cooper, A. 1976. Thermodynamic fluctuations in protein molecules. *Proc. Natl. Acad. Sci. USA.* 73:2740–2741.
6. Evans, G. J., M. W. Evans, and R. Pething. 1982. The far infrared spectra of proteins and enzymes in the solid state. *Spectrochim. Acta. Part A Mol. Spectrosc.* 38:421–422.
7. Wanger, C. 1982. Internal mobility in globular proteins. *Comments Mol. Cell. Biophys.* 1:261–280.
8. Green, D. E. 1974. Framework on principles for the unification of bioenergetics. *Ann. NY. Acad. Sci.* 227:6–45.
9. Ji, S. 1974. Energy and negentropy in enzyme catalysts. *Ann. NY. Acad. Sci.* 227:419–437.
10. Fröhlich, H. 1975. The extraordinary dielectric properties of biological materials and the action of enzymes. *Proc. Natl. Acad. Sci. USA.* 72:4211–4215.
11. Suezaki, Y., and N. Gō. 1975. Breathing mode of conformational fluctuations in globular proteins. *Int. J. Pept. Protein Res.* 7:333–334.
12. Ponnuswamy, P. K., and R. Bhaskaran. 1982. Internal fluctuations in globular proteins. *Int. J. Pept. Protein Res.* 19:549–555.
13. Careri, G., P. Fasella, and E. Gratton. 1975. Statistical time events in enzyme: a physical assessment. *Crit. Rev. Biochem.* 3:141–164.

14. Englanders, S. W. 1980. Internal motions in proteins and nucleic acids and their hydrogen exchange properties. *Comments Mol. Cell. Biophys.* 1:15–28.
15. Chou, K. C., and N. Y. Chen. 1977. The biological functions of low-frequency phonons. *Sci. Sin.* 20:447–457.
16. Sobell, H. M., E. D. Lozansky, and M. Lessen. 1979. Structural and energetic considerations of wave propagation in DNA. *Cold Spring Harbor Symp. Quant. Biol.* 43:11–19.
17. Lazansky, E. D., and H. M. Sobell. 1981. The influence of acoustic phonons on the magnitude of energy fluctuations in DNA. *In* Structural Aspects of Recognition and Assembly in Biological Macromolecules. M. Balaban, editor. Balaban ISS, Rehovot and Philadelphia. 553–557.
18. Sobell, H. M., A. Banerjee, E. D. Lozansky, G. P. Zhou, and K. C. Chou. 1983. The role of low frequency (acoustic) phonons in determining the premelting and melting behavior of DNA. *In* Structure and Dynamics: Nucleic Acids and Proteins. E. Clementi and R. H. Sarma, editors. Adenine Press, New York. 181–195.
19. Zhou, G. P. 1981. Vibrational energy of ringlike DNA molecules. *Sheng Wu Hua Xue Yu Sheng Wu Wu Li Jinzhan.* 5:19–22.
20. Chou, K. C., N. Y. Chen, and S. Forsén. 1981. The biological functions of low-frequency phonons. 2. Cooperative effects. *Chem. Scr.* 18:126–132.
21. Wilson, E. B. 1939. A method of obtaining the expanded secular equation for vibration frequencies of a molecule. *J. Chem. Phys.* 7:1047–1052.
22. Itoh, K., and T. Shimanouchi. 1970. Vibrational frequencies and modes of α-helix. *Biopolymers.* 9:383–399.
23. Fanconi, B., E. W. Small, and W. L. Peticolas. 1971. Phonon dispersion curves and normal coordinate analysis of α-poly-L-alanine. *Biopolymers.* 10:1277–1298.
24. Birktoft, J. J., and D. M. Blow. 1972. Structure of crystalline α-chymotrypsin. 5. The atomic structure of tosyl-α-chymotrypsin at 2 Å resolution. *J. Mol. Biol.* 68:187–240.
25. Tang, J., P. Sepulveda, J. Marciniszyn, Jr., K. C. S. Chen, W. Y. Huang, N. Tao, D. Liu, and J. P. Lanier. 1973. Amino-acid sequence of protein pepsin. *Proc. Natl. Acad. Sci. USA.* 70:3437–3439.
26. Hsu, I. N., L. T. J. Delbaere, M. N. G. James, and T. Hofmann. 1977. Penicillo-pepsin from penicilling janthinellum crystal structure at 2.8 Å and sequence homology with porcine pepsin. *Nature (Lond.).* 266:140–145.
27. Andreeva, N. S., A. A. Fedorov, A. E. Gushchina, R. R. Riskulov, N. E. Shutskever, and M. G. Safro. 1978. X-ray structural analysis of pepsin. 5. Conformation of the main enzyme chain (Trans. from Russian). *Mol. Biol.* 12:704–716.
28. Peticolas, W. L. 1979. Mean-square amplitudes of the longitudinal vibrations of helical polymers. *Biopolymers.* 18:747–755.
29. Kresheck, G. C. 1970. Calorimetric ΔH values accompanying conformational changes of macromolecules in solution. *In* Handbook of Biochemistry. H. A. Sober, editor. The Chemical Rubber Co., Cleveland, Ohio. Section J. 74.
30. Gō, N., T. Noguti, and T. Nishikawa. 1983. Dynamics of a small globular protein in terms of low-frequency vibrational modes. *Proc. Natl. Acad. Sci. USA.* 80:3696–3700.
31. Painter, P. C., L. E. Mosher, and C. Rhoads. 1982. Low-frequency modes in the Raman spectra of proteins. *Biopolymers.* 21:1469–1472.